Quantum Chromodynamics Resolution of the ATOMKI Anomaly in $^4\mathrm{He}^* \to {}^4\mathrm{He} + \mathrm{e}^+\mathrm{e}^-$ Nuclear Transitions

Valery Kubarovsky,[1] Jennifer Rittenhouse West,[2,3] and Stanley J. Brodsky[4]

[1] *Thomas Jefferson National Accelerator Laboratory, Newport News, VA 23606, USA*
[2] *Lawrence Berkeley National Laboratory, Berkeley, CA 94720, USA*
[3] *EIC Center at Thomas Jefferson National Accelerator Laboratory, Newport News, VA 23606, USA*
[4] *SLAC National Accelerator Laboratory, Stanford University, Stanford, CA 94309, USA*

(Dated: Monday 13th June, 2022)

Recent observations of a narrow peak in the $m_{e^+e^-}$ invariant mass spectra in the nuclear decays $^8\mathrm{Be}^* \to {}^8\mathrm{Be} + \mathrm{e}^+\mathrm{e}^-$ and $^4\mathrm{He}^* \to {}^4\mathrm{He} + \mathrm{e}^+\mathrm{e}^-$ have been suggested as due to the creation and subsequent decay to an electron-positron pair of a new light particle with a mass of ~ 17 MeV. In this work, we present the calculation of the invariant mass $m_{e^+e^-}$ spectrum in the electromagnetic transition process of an excited state of ^{4}He, $^4\mathrm{He}^*(\mathrm{E}^*) \to {}^4\mathrm{He} + \gamma^* \to {}^4\mathrm{He} + \mathrm{e}^+\mathrm{e}^-$, where E* is the excited state energy, and estimate the differential and total width of this decay. We investigate the possibility of a new electromagnetic transition in the helium nucleus due to the proposed 12-quark color singlet Fock state in the ^{4}He nuclear wavefunction (the "hexadiquark") as the source of the signal and find we can fit the shape of the signal with a Gaussian form factor and a new excited state of ^{4}He at ~ 17.9 MeV. We address the physical issues with the fit parameters using QCD-based hexadiquark transitions. In light of this work, we emphasize the need for independent experimental confirmation or refutation of the ATOMKI results as well as further experiments to detect the proposed new excitation of ^{4}He.

Introduction

The observation of a narrow peak in the electron-positron pair invariant mass spectra by the ATOMKI collaboration in the nuclear decays $^8\mathrm{Be}^* \to {}^8\mathrm{Be} + \mathrm{e}^+\mathrm{e}^-$ [1] and $^4\mathrm{He}^* \to {}^4\mathrm{He} + \mathrm{e}^+\mathrm{e}^-$ [2, 3] may be explained by the creation and subsequent decay to an e^+e^- pair of a new light particle with mass of ~ 17 MeV, dubbed the X17 or simply X. Recently the same group reported observations of the X17 anomaly in the $^7\mathrm{Li}(\mathrm{p}, \mathrm{e}^+\mathrm{e}^-)^8\mathrm{Be}$ direct proton-capture reaction [4]. Our work focuses on the ^{4}He experimental data in which the precise mass was found to be $m_\mathrm{X} = 16.94 \pm 0.12(\text{ stat. }) \pm 0.21$ (syst.) MeV. The Feynman diagram for this transition is shown in Fig. 1. Experimentally the signal is a narrow Gaussian peak with a mean value ~ 17 MeV and $\sigma \sim 0.7$ MeV (see Fig. 2). The peak has generated a great deal of theoretical interest in both the particle and nuclear physics communities [5–19].

In this work on the ATOMKI anomalies, we present a successful QCD-based fit to their data. We begin with a calculation of the invariant mass $m_{e^+e^-}$ spectrum in the electromagnetic transition of an excited state of ^{4}He, $^4\mathrm{He}^*(\mathrm{E}^*) \to {}^4\mathrm{He} + \gamma^* \to {}^4\mathrm{He} + \mathrm{e}^+\mathrm{e}^-$, where E* is the excited state energy. The mass difference between the first known excited state and the ground state of the helium nucleus is 20.21 MeV [20] and E* is initially fixed to this value. It is subsequently allowed to float due to the possibility of the new 12-quark Fock state in the ^{4}He nuclear wavefunction [21]. The spin-parity of the excited state $^4\mathrm{He}^*(20.21)$ and ground state ^{4}He is $J^P = 0^+$ which simplifies the calculation of the matrix element previously carried out [11]. The invariant mass $m_{e^+e^-}$ distribution has not been calculated until now. The results of our calculations show that excitations caused by the hexadiquark Fock state in the nuclear wavefunction of ^{4}He can describe the observed signal and, in fact, are to be expected from this new "hidden color" QCD state.

Nuclear decay amplitude for $^4\mathrm{He}^* \to {}^4\mathrm{He} + e^+e^-$

The square of the amplitude for the electromagnetic decay $^4\mathrm{He}^* \to {}^4\mathrm{He} + e^+e^-$ is [11] is given by

$$|\mathcal{M}|^2 = \sum_{\text{spin}} |M|^2 = \frac{e^4\, C_{\mathrm{E0}}^2}{\Lambda^4} \left[2(p_+ \cdot p_0)(p_- \cdot p_0) - m_0^2(p_+ \cdot p_-) - m_e^2 m_0^2\right], \tag{1}$$

where p_+ and p_- are the 4-momenta of the positron and electron respectively, p_0 and m_0 are the 4-momentum and mass of the ground state of ^{4}He, m_e is the electron mass and final state spins have been summed over. The definitions of Λ as the nuclear energy scale and C_{E0}^2 as the Wilson coefficient of the decay operator are contained in [11]. These

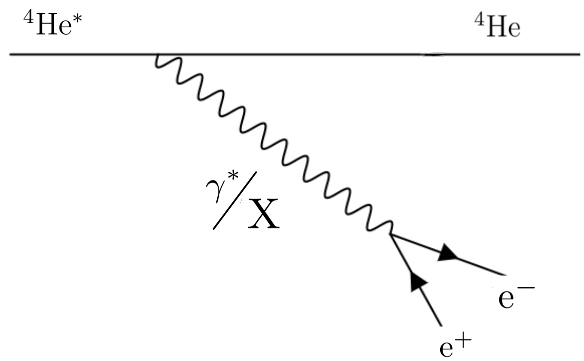

FIG. 1. Feynman diagram for the electromagnetic/X-boson transition $^4\text{He}^* \to {}^4\text{He} + e^+e^-$.

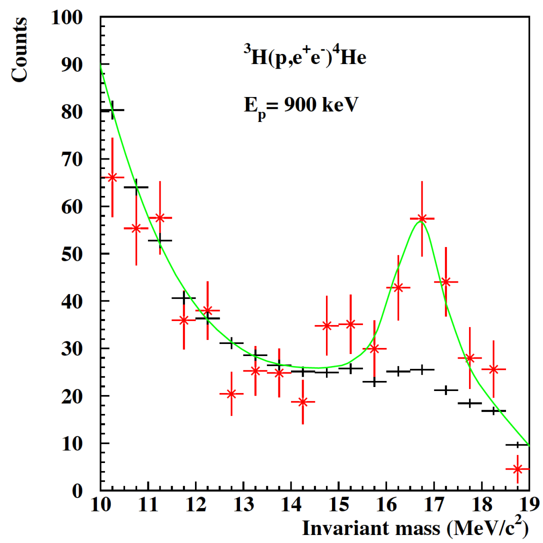

FIG. 2. Invariant mass $m_{e^+e^-}$ distribution in the nuclear decay $^4\text{He}^* \to {}^4\text{He} + \text{e}^+\text{e}^-$ from [2, 3]. Error bars are 1σ. The signal is in red, the background is black.

constants are not relevant for the analysis carried out in this work.

The matrix element depends on only two kinematical variables, q^2 and $\cos\theta^*$, where $q = p_+ + p_-$ is the 4-momentum of the virtual photon, $q^2 = m^2_{e^+e^-}$ is the e^+e^- invariant mass squared and θ^* is the electron angle in the virtual photon center of mass system. Rewriting Eq.1 in terms of these variables gives

$$\left|\mathcal{M}(q^2, \cos\theta^*)\right|^2 = \frac{\alpha^2 C^2_{E0}}{\Lambda^4} \frac{(4\pi)^2}{8q^2} \left[q^2 - \cos^2\theta^*(q^2 - 4m_e^2)\right] \left[m^4 + (m_0^2 - q^2)^2 - 2m(m_0^2 + q^2)\right] \quad (2)$$

where m is the mass of the excited $^4\text{He}^*$ state.

The differential width $d\Gamma$ for the three body decay is given by

$$d\Gamma = \frac{1}{(2\pi)^5} \frac{1}{16m^2} \left|\mathcal{M}\right|^2 |p_e^*||p_0| dm_{e^+e^-} d\Omega_e^* d\Omega_0 \quad (3)$$

where $d\Omega = d\phi \; d\cos\theta$, $(|p_e^*|, \Omega_e^*)$ is the electron momentum in the center of mass of the electron-positron pair,

$(|p_0|, \Omega_0)$ is the ^{4}He momentum in the rest frame of the ^{4}He*.

The $|p_e^*||p_0|$ product in terms of the kinematical variables is

$$|p_e^*||p_0| = \frac{\sqrt{(q^2 - 4m_e^2)\,(m^2 - (m_0 - q)^2)\,(m^2 - (m_0 + q)^2)}}{4m} \tag{4}$$

and is plotted in Fig. 3. The minimum value of the $m_{e^+e^-}$ invariant mass is $2m_e$ and maximum value is determined by the mass difference between excited and ground ^{4}He states Δm =20.21 MeV.

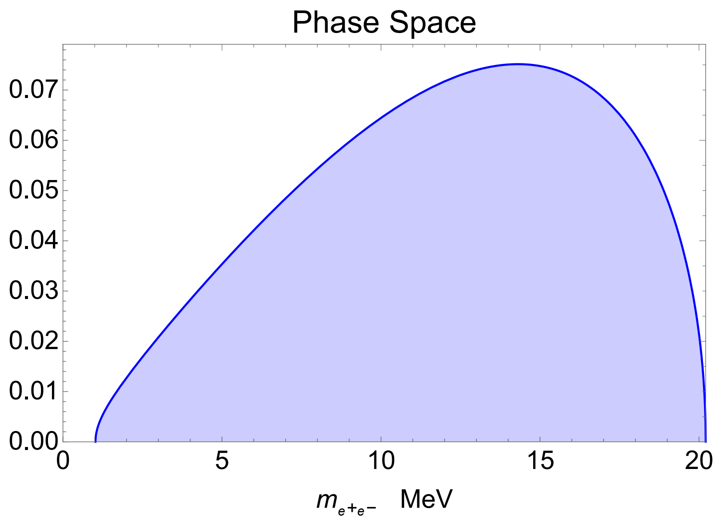

FIG. 3. The phase space $|p_e^*||p_0|$ of the process ^{4}He$^* \to {}^4$He $+ e^+e^-$.

The maximum value for the ratio $q^2/m^2 < (m - m_0)^2/m^2 = 3 \cdot 10^{-5} \ll 1$. Taking into account this small ratio and in the limit $m_e = 0$ the phase space becomes

$$|p_e^*||p_0| = \frac{q}{2}\sqrt{\Delta m^2 - q^2}. \tag{5}$$

The integration of the matrix element $\left|\mathcal{M}(q^2, \cos\theta^*)\right|^2$ over angles $d\Omega_e^*\Omega_0$ gives

$$\left|\mathcal{M}_q(q^2)\right|^2 = \int \left|\mathcal{M}(q^2, \cos\theta^*)\right|^2 d\Omega_e^* d\Omega_0 = \frac{\alpha^2 C_{E0}^2}{\Lambda^4}\frac{(4\pi)^4}{12q^2}(q^2 + 2m_e^2)\left[m^4 + (m_0^2 - q^2)^2 - 2m^2(m_0^2 + q^2)\right]. \tag{6}$$

The matrix element $\left|\mathcal{M}_q(q^2)\right|^2$ is simplified in the limit $m_e = 0$, to become

$$\left|\mathcal{M}_q(q^2)\right|^2 = \frac{\alpha^2 C_{E0}^2}{\Lambda^4}\frac{(4\pi)^4}{12}\left[m^4 + (m_0^2 - q^2)^2 - 2m^2(m_0^2 + q^2)\right]. \tag{7}$$

There is only one variable left, the invariant electron-positron mass $m_{e^+e^-} = \sqrt{q^2} = \sqrt{(p_+ + p_-)^2}$, and we find

$$d\Gamma = \frac{1}{(2\pi)^5}\frac{1}{16m^2}\left|\mathcal{M}_q\right|^2 |p_e^*||p_0| dm_{e^+e^-}. \tag{8}$$

The numerical integration over the three-body phase space is

$$\Gamma_{E0} = \int_{2m_e}^{m-m_0} dm_{e^+e^-}\left|\mathcal{M}_q(q^2)\right|^2 |p_e^*||p_{He}| = \frac{\alpha^2 C_{E0}^2}{\Lambda^4}\;(7.0627\ \text{MeV})^5. \tag{9}$$

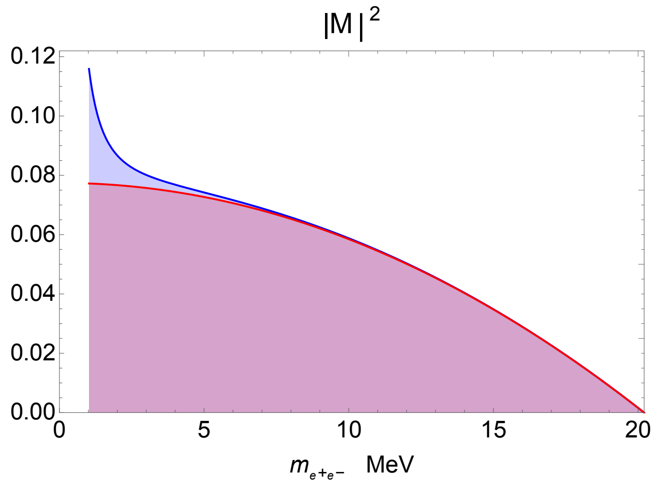

FIG. 4. The matrix element $\left|\mathcal{M}_q(q^2)\right|^2$ for the process ${}^4\text{He}^* \to {}^4\text{He} + e^+e^-$. Blue: Exact result, Red: The calculation in the limit $m_e \to 0$.

We can rewrite it in more convenient way

$$\Gamma_{E0} = \int_{2m_e}^{m-m_0} dm_{e^+e^-} \left|\mathcal{M}_q(q^2)\right|^2 |p_e^*||p_{He}| = \frac{\alpha^2 C_{E0}^2}{\Lambda^4} \frac{\Delta m^5}{60\pi} 0.982, \tag{10}$$

and with an accuracy of 2% this coincides with the approximate solution (Eq. 13, below).

In the approximation $q^2/m^2 < \Delta m^2/m^2 = 3 \cdot 10^{-5} \ll 1$, the matrix element and differential width $d\Gamma/dm_{e^+e^-}$ are

$$|\mathcal{M}_q(q^2)|^2 = \frac{\alpha^2 C_{E0}^2}{\Lambda^4} \frac{(4\pi)^4}{3} m^2 \left[\Delta m^2 - q^2\right] \tag{11}$$

and

$$\frac{d\Gamma}{dm_{e^+e^-}} = \frac{\alpha^2 C_{E0}^2}{12\pi\Lambda^4} \; m_{e^+e^-} \left(\Delta m^2 - m_{e^+e^-}^2\right)^{\frac{3}{2}}. \tag{12}$$

The full width has an analytic solution in this case,

$$\begin{aligned} \Gamma_{E0} &= \frac{\alpha^2 C_{E0}^2}{12\pi\Lambda^4} \int_{2m_e}^{m-m_0} m_{e^+e^-} \left(\Delta m^2 - m_{e^+e^-}^2\right)^{\frac{3}{2}} dm_{e^+e^-} \\ &= \frac{\alpha^2 C_{E0}^2}{\Lambda^4} \frac{\left(\Delta m^2 - 4m_e^2\right)^{\frac{5}{2}}}{60\pi} \approx \frac{\alpha^2 C_{E0}^2}{\Lambda^4} \frac{\Delta m^5}{60\pi} \end{aligned} \tag{13}$$

that with 2% accuracy corresponds to the exact solution of Eq. 10.

The matrix element from Eq. 6 (exact solution) and Eq. 7 (approximation with m_e=0), integrated over $\cos\theta^*$ and normalized to one, is presented in Fig. 4.

The unintegrated matrix element (Eq. 2) for two values, $\cos\theta^* = 0$ and $\cos\theta^* = 1$, is presented in Fig. 5. The experimental data [2, 3] were taken with $\cos\theta^* \sim 0$. There is no evidence for any structure near $m_{e^+e^-} = 17$ MeV in both Fig. 4 and 5.

The differential width $d\Gamma/dm_{e^+e^-}$ from Eq. 2, integrated over $\cos\theta^*$ and normalized to one, is presented in Fig. 6. The distribution is very smooth from the minimum value of $m_{e^+e^-} = 2m_e$ up to maximum Δm =20.21 MeV. Thus we conclude that the ATOMKI signal cannot arise from the straightforward analysis carried out in this section.

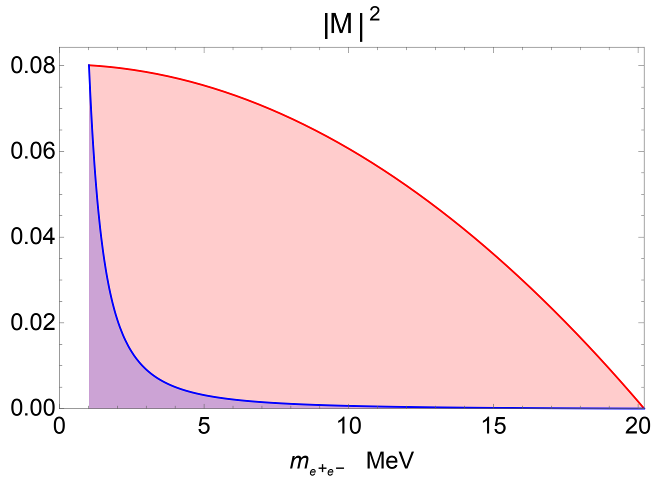

FIG. 5. The matrix element $|\mathcal{M}(q, \cos\theta^*)|^2$ squared for the process ${}^4\mathrm{He}^* \to {}^4\mathrm{He} + \mathrm{e}^+\mathrm{e}^-$. Red: $\cos\theta^* = 0$, Blue: $\cos\theta^* = 1$.

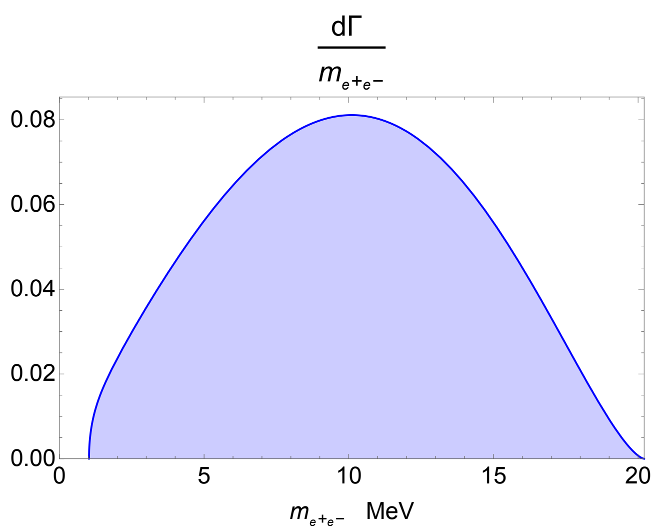

FIG. 6. The differential width $d\Gamma/dm_{e^+e^-}$ for the process ${}^4\mathrm{He}^* \to {}^4\mathrm{He} + e^+e^-$.

Electromagnetic transition form factors $F(q^2)$ in the reaction ${}^4\mathrm{He}^* \to {}^4\mathrm{He} + e^+e^-$

The analysis carried out in the previous section implicitly assumed a form factor $F(q^2)$ equal to unity. A more realistic $F(q^2)$ could significantly change the $m_{e^+e^-}$ invariant mass distribution in the nuclear decay ${}^4\mathrm{He}^* \to {}^4\mathrm{He} + e^+e^-$. The amplitude squared with the explicit form factor is given by

$$|\mathcal{M}|^2 = \sum_{\text{spin}} |M|^2 = \frac{e^4\, C_{\mathrm{E0}}^2}{\Lambda^4} \left[2(p_+ \cdot p_0)(p_- \cdot p_0) - m_0^2(p_+ \cdot p_-) - m_e^2 m_0^2\right] \left|F(q^2)\right|^2 . \tag{14}$$

The experimental $m_{e^+e^-}$ distribution is not given in the published paper. In order to compare the theoretical work in this section to the data, we first extract the ATOMKI data, plot them and confirm that we can replicate their results. To this end, we've used the extracted signal and background distributions from Fig. 2 and made a fit with two functions to describe the signal observed in the experiment and background distributions. Fig. 7 presents our fit with a Gaussian function to describe the signal. The background was fitted independently because the experiment measured the background distribution with much higher accuracy than the signal. The fit has 3 parameters: the peak position, σ and overall normalization. Our fit is very close to the published one (see Fig. 2). The differences are very small and do not affect our conclusions. We are confident that this procedure was carried out correctly and can move onto fitting the results theoretically.

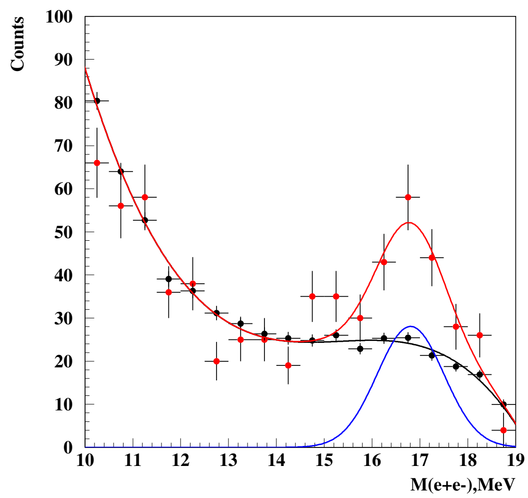

FIG. 7. Fit by Gaussian function (in red) and background distribution (in black) of the published ATOMKI $m(e^+e^-)$ invariant mass distribution. The signal alone is shown in blue.

Several realistic form factor models are tested in our attempt to model the experimental data. Fig. 8 presents the comparison of the differential width $d\Gamma/dm_{e^+e^-}$ for the electromagnetic transition with form factor $F(q^2) = 1$ (in blue) and with $F(q^2) \propto q^2$. The low mass region is indeed suppressed by the form factor and the distribution has a peak near the value of $m_{e^+e^-} = 17$ MeV. However the comparison with the experimental signal, shown in black, suggests that the width of the curve with $F(q^2) \propto q^2$ is much larger in comparison to the Gaussian peak (m =17 MeV, σ =0.7 MeV) published by the ATOMKI group.

Fig.9 presents the result of the fit with an electromagnetic transition form factor $F(q^2) \propto q^2$. The background function is the same as in Fig. 7. This fit has only one parameter, the normalization factor of the theoretical function. The fit is not satisfactory. The observed signal is too narrow in comparison with the theoretical curve as it is shown in the Fig. 8, compare red plot (theoretical curve) and black curve (experimentally observed signal).

Fig. 10 presents the comparison of the differential width $d\Gamma/dm_{e^+e^-}$ for the electromagnetic transition with form factor $F(q^2) = 1$ (in blue) and with $F(q^2) \propto \exp -(q/\lambda)^2$ with $\lambda = 11$ MeV. As in the case with form factor $F(q^2) \propto q^2$, we can get a distribution with the maximum near 17 MeV. However the width of the distribution is too large to obtain a satisfactory description of the experimental distribution.

Fig.11 presents the result of the fit with electromagnetic transition form factor $F(q^2) \propto \exp -(q/\lambda)^2$. The background function is the same as in Fig. 7. This fit has two parameters, $\lambda = 11 \pm 1$ MeV and the normalization factor of the theoretical function. The fit is not satisfactory. The observed signal is too narrow in comparison with the theoretical curve as it is shown in the Fig. 10, comparing the red plot (theoretical curve) and black curve (experimentally observed signal).

One of the reasons for the unsatisfactory fit to the data with different form factor models is the position and width of the X17 signal. The X17 mass is 4σ away from the kinematical limit 20.21 MeV. If the signal is coming from the decay of new excited $^4\mathrm{He}^*$ state with mass difference of 18 MeV the fit will be successful. This situation is realized in the decay $^8\mathrm{Be}^* \to {}^8\mathrm{Be} + \mathrm{e}^+\mathrm{e}^-$ [1] where the mass difference between excited state and the ground state is only 18.15 MeV. The ^{8}Be ATOMKI enhancement has been described by an electromagnetic transition with a form factor included [12]. The momentum scale of the form factor was around 20 MeV with a length scale on the order of tens of fm. The authors of that work noted that the natural form factor scale should be close to 200 MeV, the QCD energy scale. This differs by an order of magnitude from the fit to the experimental data.

We now introduce a new parameter, the mass of a new excited $^4\mathrm{He}^*$ state, into our model. We motivate this state by the proposed 12-quark color singlet Fock state model of ^{4}He nucleus in which the ^{4}He wavefunction is dominated by a linear combination of $|nnpp\rangle$ and the 12-quark "hexadiquark" QCD state [21]. The result of the fit with form factor $F(q^2) \propto \exp -(q/\lambda)^2$ is presented in Fig. 12. There are three parameters of the fit, the mass of the new excited state ^{4}He* $m = 17.9 \pm 1$ MeV, the form factor parameter $\lambda = 6.2 \pm 0.2$ MeV and the overall normalization. The model describes the data very well. Our parameter $\lambda = 6.2 \pm 0.2$ MeV is close to the momentum scale found in earlier work on nuclear transitions [12]. We have managed to describe the ATOMKI signal with the introduction of a new excited ^{4}He$^*(17.9)$ state but there are serious physical issues that must be addressed. First, the energy of the electron-positron pair in this case has to be 17.9 MeV with high accuracy. This is 1.6σ away from the lower limit of the selection of the positrons and electrons with total energy in the region (19.5, 22.0) MeV and is a state that has never been observed. In addition, the form factor parameter λ is an order of magnitude smaller than expected for a typical nuclear transition. We address both of these points in the following section.

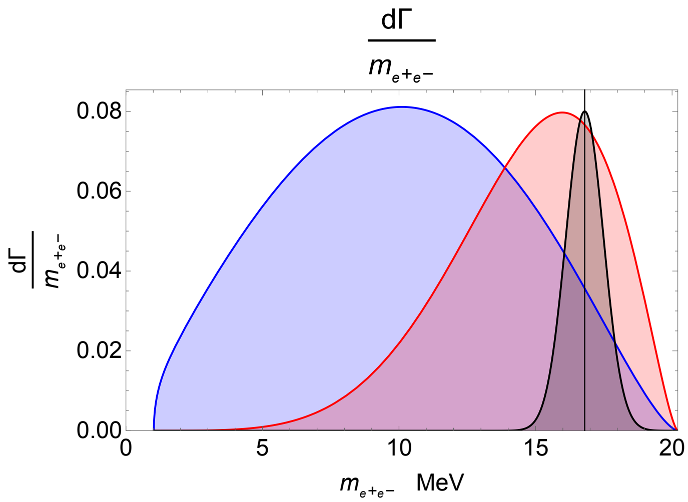

FIG. 8. The differential width $d\Gamma/dm_{e^+e^-}$ for the transition ^{4}He$^*(20.21) \to {}^4$He$+ e^+e^-$. Blue: $F(q^2) = 1$, Red: $F(q^2) \propto q^2$, Black: Gaussian distribution with m =17 MeV and σ =0.7 MeV. The functions are normalized such that the peak values are the same for all curves.

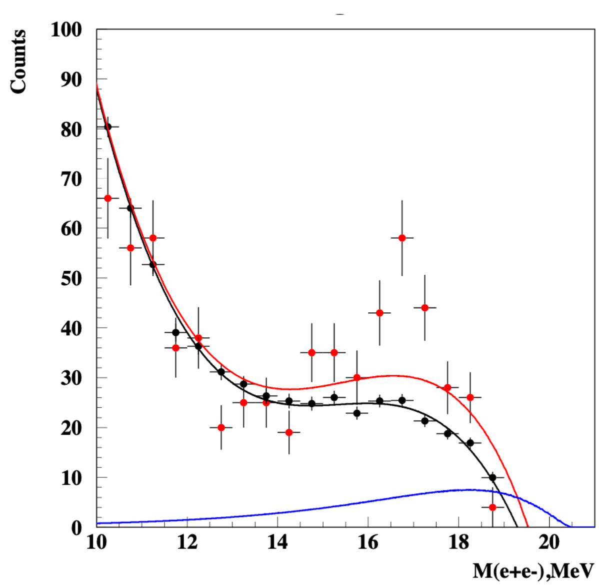

FIG. 9. Fit by electromagnetic transition function with form factor $F(q^2) \propto q^2$ (in red) and background distribution (in black). The signal alone is shown in blue.

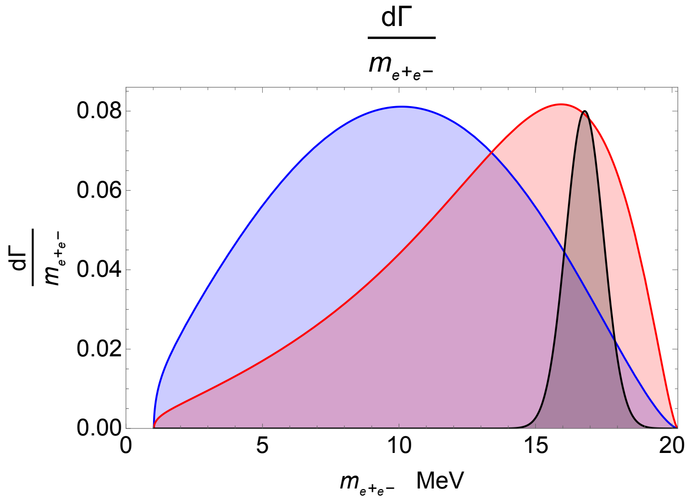

FIG. 10. The differential width $d\Gamma/dm_{e^+e^-}$ for the transition ${}^4\mathrm{He}^*(20.21) \to {}^4\mathrm{He} + e^+e^-$. Blue: $F(q^2) = 1$ Red: $F(q^2) \propto \exp -(q/\lambda)^2$ with $\lambda = 11$ MeV.

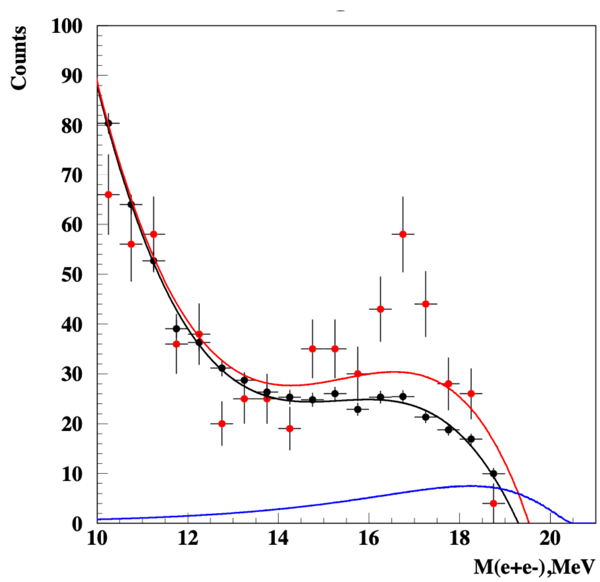

FIG. 11. Fit by electromagnetic transition function with form factor $F(q^2) \propto \exp -(q/\lambda)^2$ (in red) and background distribution (in black). The signal alone is shown in blue.

Hexadiquark excitations

The hexadiquark (HdQ) is a "hidden color" [23, 24] QCD state in the ^{4}He nuclear wavefunction [21] consisting of six scalar $[ud]$ diquarks [25, 26] in a color singlet configuration. Excitation of a subset of diquarks, either radial or angular momentum excitations, can give rise to nuclear transitions with unconventional decays. To illustrate this, we consider the electron scattering experiment $e + {}^4\mathrm{He} \to e' + X$.

In conventional nuclear physics, the collision will produce hadronic excitations of ^{4}He, e.g., a proton + tritium, in an excited radial or orbital state: $e + {}^4\mathrm{He} \to e' + {}^4\mathrm{He}^* \to e' + p + {}^3\mathrm{H}$. Similarly, conventional nuclear physics excitations ${}^4\mathrm{He}^*$ can be observed in a proton beam experiment, such as $p + {}^4\mathrm{He} \to p' + {}^4\mathrm{He}^*(20.21) \to p' + p'' + {}^3\mathrm{H}$. However, if an electron or proton scatters on the hexadiquark Fock state of ^{4}He, it can produce orbital or radial excitations between

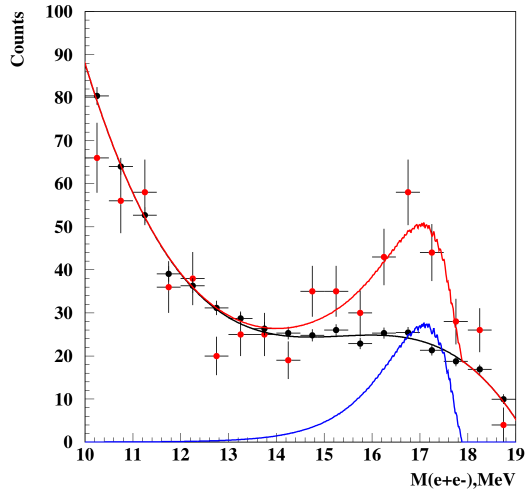

FIG. 12. Fit by electromagnetic transition function $^4\mathrm{He}^*(17.9) \to {}^4\mathrm{He} + (\mathrm{e}^+\mathrm{e}^-)$ with form factor $F(q^2) \propto \exp -(q/\lambda)^2$ (in red) and background distribution (in black). The signal alone is shown in blue.

any two of the [ud] diquarks; e.g. $([ud] + [ud]) + [[ud][ud][ud][ud]]$. Typically such excitations would be at energies near 300 MeV, in analogy to the N^* and Δ excited states of nucleons. Excitations of single diquarks from spin-0 isospin-0 to spin-1 isospin-1 have energies of the order 100 MeV. However, the HdQ is an unusual QCD state because it is built with three symmetric and *repulsive* $\bar{3} \times \bar{3} \to \bar{6}$ of $\mathrm{SU(3)_C}$ interactions at the duodiquark stage of the build, $[ud][ud]$. While the full build of the HdQ is strongly bound with color factor $C_F = -5$, the QCD potential between diquarks in a duodiquark is repulsive and given by $V(r) = -\frac{1}{3}\frac{g_s^2}{4\pi r}$. An $L = 1$ excitation between diquarks in the repulsive duodiquark is a viable low mass excitation. (This is in contrast to the strongly bound attractive $3 \times \bar{3} \to 1$ of the quark-diquark bond in baryons, with short-range QCD potential $V(r) = +\frac{4}{3}\frac{g_s^2}{4\pi r}$.) Such a color-singlet excitation of the HdQ would not easily decay to a conventional nuclear physics state; however, it can decay to the ^{4}He ground state by emitting a virtual photon which makes an e^+e^- pair. The HdQ thus could be the origin of a previously missed $^4\mathrm{He}^*(17.9)$ excited state. It can be observed in $e + {}^4\mathrm{He} \to e' + {}^4\mathrm{He}^*(17.9) \to e' + {}^4\mathrm{He} + [e^+e^-]$.

The mass scale of the transition form factor $F(q^2)$ producing the timelike lepton pair $\mathrm{HdQ}^* \to \mathrm{HdQ} + \gamma^*$ should be small, since it reflects the large size structure of the HdQ and its excitations such as $[ud][[ud] + [ud][ud][ud][ud]]$, allowing for the λ parameter of order 10 MeV as our fit requires. The spin-parity of the lepton pair could be either $J^{PC} = 0^{++}$ or 1^{--}. In either case, $F(q^2 = 0) = 0$. The conclusion from these arguments is that an excitation of the HdQ can account for the excellent fit and parameters in Fig.12 to the ATOMKI data given in Fig.7. We note that the hexadiquark state has been proposed as a hidden color state within every nucleus containing an alpha particle and therefore this decay will also be observed in ^{9}Be and ^{12}C.

We propose tests of the HdQ description of the ATOMKI signals. The hexadiquark composition of ^{4}He could be observed as a peak in the missing mass in $e + {}^4\mathrm{He} \to \mathrm{e}' + \mathrm{X}$ and by observing $e + {}^4\mathrm{He} \to \mathrm{e}' + [\mathrm{ud}] + \mathrm{X}$ which produces a $[ud]$-diquark jet [22] opposite the scattered electron.

Conclusions

We have presented a hidden color QCD solution to the ATOMKI anamoly. The calculation of the invariant mass $m_{e^+e^-}$ spectrum in the electromagnetic transition process $^4\mathrm{He}^*(E^*) \to {}^4\mathrm{He} + \gamma^* \to {}^4\mathrm{He} + e^+e^-$ and the estimated the differential and total width of the decay can be fit by new diquark excitations of ^{4}He. Taking into account the small mass difference Δm between the excited and ground states of the ^{4}He nuclei in comparison with the nuclear mass $(m - m_0)^2/m^2 = 3 \cdot 10^{-5} \ll 1$, we found a simple expression for the differential width of this decay

$$\frac{d\Gamma}{dm_{e^+e^-}} \propto m_{e^+e^-} \left(\Delta m^2 - m^2_{e^+e^-}\right)^{\frac{3}{2}}.$$

The total width depends only on the mass difference $\Gamma_{E0} \propto \Delta m^5$ in the limit of negligible electron mass. The $m_{e^+e^-}$ distribution is a smooth function between the limits of $2m_e$ and Δm. We've demonstrated that it is not possible to describe the published ATOMKI excesses [1] by the electromagnetic decay $^4\text{He}^*(20.21) \to {}^4\text{He} + \gamma^* \to {}^4\text{He} + e^+e^-$. While introducing a form factor to the electromagnetic transition with definite parameters creates a peak close to 17 MeV as required, the width of the distribution is different from the experimental value $\sigma = 0.7$ MeV. This attempt to fit ATOMKI data with various plausible form factor models fails to describe the experimental data.

It is possible to obtain the shape of the ATOMKI signal by introducing a new excited $^4\text{He}^*$ state with mass 17.9 MeV above the ground state, motivated by the proposed color singlet hexadiquark Fock state model of the nuclear wavefunction of ^{4}He [21]. The energy of the electron-positron pair in this case has to be very close to 17.9 MeV, a value which is 1.6σ from the lower limit of the selection of the positrons and electrons with energy in the region (19.5, 22.0) MeV. While the nuclear energy scale for a ^{4}He decay is of the order $\lambda \sim 200$ MeV, an order of magnitude larger than the energy coming from our fit, excitations of the three repulsive interaction duodiquarks within the hexadiquark state are naturally at these energy and length scales. The existence of the ATOMKI X17 lepton pair events requires that there must also be a peak near 17.9 MeV in ^{4}He.

Acknowledgements

V.K. acknowledges support by the U.S. Department of Energy, Office of Science, Office of Nuclear Physics under contracts DE- AC05-06OR23177. J.R.W. acknowledges partial support from the LDRD program of Lawrence Berkeley National Laboratory and the EIC Center at Thomas Jefferson National Accelerator Laboratory. SLAC-PUB-17683.

[1] A.J. Krasznahorkay et al., Phys. Rev. Lett. 116, 042501, (2016).
[2] A. J. Krasznahorkay, M. Csatlós, L. Csige, J. Gulyás, A. Krasznahorkay, B. M. Nyakó, I. Rajta, J. Timár, I. Vajda and N. J. Sas, Phys. Rev. C **104**, no.4, 044003 (2021) doi:10.1103/PhysRevC.104.044003 [arXiv:2104.10075 [nucl-ex]].
[3] A.J. Krasznahorkay, M. Csatlos, L. Csige et al. arXiv:1910.10459 [nucl-ex], (2019).
[4] N. J. Sas, A. J. Krasznahorkay, M. Csatlós, J. Gulyás, B. Kertész, A. Krasznahorkay, J. Molnár, I. Rajta, J. Timár and I. Vajda, *et al.* [arXiv:2205.07744 [nucl-ex]].
[5] M. Battaglieri, A. Belloni, A. Chou, P. Cushman, B. Echenard, R. Essig, J. Estrada, J. L. Feng, B. Flaugher and P. J. Fox, *et al.* [arXiv:1707.04591 [hep-ph]].
[6] B. Fornal, Int. J. Mod. Phys. A **32**, 1730020 (2017) doi:10.1142/S0217751X17300204 [arXiv:1707.09749 [hep-ph]].
[7] P. Agrawal, M. Bauer, J. Beacham, A. Berlin, A. Boyarsky, S. Cebrian, X. Cid-Vidal, D. d'Enterria, A. De Roeck and M. Drewes, *et al.* Eur. Phys. J. C **81**, no.11, 1015 (2021) doi:10.1140/epjc/s10052-021-09703-7 [arXiv:2102.12143 [hep-ph]].
[8] J. Alexander, M. Battaglieri, B. Echenard, R. Essig, M. Graham, E. Izaguirre, J. Jaros, G. Krnjaic, J. Mardon and D. Morrissey, *et al.* [arXiv:1608.08632 [hep-ph]].
[9] J. Kozaczuk, D. E. Morrissey and S. R. Stroberg, Phys. Rev. D **95**, no.11, 115024 (2017) doi:10.1103/PhysRevD.95.115024 [arXiv:1612.01525 [hep-ph]].
[10] T. Kitahara and Y. Yamamoto, Phys. Rev. D **95**, no.1, 015008 (2017) doi:10.1103/PhysRevD.95.015008 [arXiv:1609.01605 [hep-ph]].
[11] J. Feng, T. Tait and C. Verhaaren, Phys. Rev. D **102**, no.3, 036016 (2020) doi:10.1103/PhysRevD.102.036016 [arXiv:2006.01151 [hep-ph]].
[12] X. Zhang and G. A. Miller, Phys. Lett. B **773**, 159-165 (2017) doi:10.1016/j.physletb.2017.08.013 [arXiv:1703.04588 [nucl-th]].
[13] X. Zhang and G. A. Miller, Phys. Lett. B **813**, 136061 (2021) doi:10.1016/j.physletb.2021.136061 [arXiv:2008.11288 [hep-ph]].
[14] C. Frugiuele, E. Fuchs, G. Perez and M. Schlaffer, Phys. Rev. D **96**, no.1, 015011 (2017) doi:10.1103/PhysRevD.96.015011 [arXiv:1602.04822 [hep-ph]].
[15] L. Delle Rose, S. Khalil, S. J. D. King and S. Moretti, Front. in Phys. **7**, 73 (2019) doi:10.3389/fphy.2019.00073 [arXiv:1812.05497 [hep-ph]].
[16] D. Banerjee *et al.* [NA64], Phys. Rev. Lett. **120**, no.23, 231802 (2018) doi:10.1103/PhysRevLett.120.231802 [arXiv:1803.07748 [hep-ex]].

[17] J. A. Dror, R. Lasenby and M. Pospelov, Phys. Rev. Lett. **119**, no.14, 141803 (2017) doi:10.1103/PhysRevLett.119.141803 [arXiv:1705.06726 [hep-ph]].
[18] D. S. M. Alves and N. Weiner, JHEP **07**, 092 (2018) doi:10.1007/JHEP07(2018)092 [arXiv:1710.03764 [hep-ph]].
[19] A. Ariga *et al.* [FASER], Phys. Rev. D **99**, no.9, 095011 (2019) doi:10.1103/PhysRevD.99.095011 [arXiv:1811.12522 [hep-ph]].
[20] T. Walcher, Phys. Lett. B **31**, 442-444 (1970) doi:10.1016/0370-2693(70)90148-6
[21] J. Rittenhouse West, S. J. Brodsky, G. F. de Teramond, A. S. Goldhaber and I. Schmidt, Nucl. Phys. A **1007**, 122134 (2021) doi:10.1016/j.nuclphysa.2020.122134 [arXiv:2004.14659 [hep-ph]].
[22]
[22] E. M. Ilgenfritz, J. Kripfganz and A. Schiller, "Fragmentation of Quark and Diquark Jets," Acta Phys. Polon. B **9**, 881 (1978) KMU-HEP-7802.
[23] S. J. Brodsky, C. R. Ji and G. P. Lepage, Phys. Rev. Lett. **51**, 83 (1983) doi:10.1103/PhysRevLett.51.83
[24] S. J. Brodsky and B. T. Chertok, Phys. Rev. D **14**, 3003-3020 (1976) doi:10.1103/PhysRevD.14.3003
[25]
[25] R. L. Jaffe, "Exotica," Phys. Rept. **409**, 1-45 (2005) doi:10.1016/j.physrep.2004.11.005 [arXiv:hep-ph/0409065 [hep-ph]].
[26] J. Rittenhouse West, [arXiv:2009.06968 [hep-ph]].